NASA TECHNICAL NOTE

NASA TN D-7005

ABLATION PERFORMANCE OF GLASSLIKE CARBONS, PYROLYTIC GRAPHITE, AND ARTIFICIAL GRAPHITE IN THE STAGNATION PRESSURE RANGE 0.035 TO 15 ATMOSPHERES

by Howard G. Maahs

Langley Research Center
Hampton, Va. 23365

NATIONAL AERONAUTICS AND SPACE ADMINISTRATION • WASHINGTON, D. C. • DECEMBER 1970

1. Report No. NASA TN D-7005	2. Government Accession No.	3. Recipient's Catalog No.
4. Title and Subtitle ABLATION PERFORMANCE OF GLASSLIKE CARBONS, PYROLYTIC GRAPHITE, AND ARTIFICIAL GRAPHITE IN THE STAGNATION PRESSURE RANGE 0.035 TO 15 ATMOSPHERES		5. Report Date December 1970 6. Performing Organization Code
7. Author(s) Howard G. Maahs		8. Performing Organization Report No. L-7290
9. Performing Organization Name and Address NASA Langley Research Center Hampton, Va. 23365		10. Work Unit No. 124-07-18-06 11. Contract or Grant No.
12. Sponsoring Agency Name and Address National Aeronautics and Space Administration Washington, D.C. 20546		13. Type of Report and Period Covered Technical Note 14. Sponsoring Agency Code
15. Supplementary Notes		

16. Abstract

The ablation performance of two glasslike carbons, one pyrolytic graphite, and one artificial graphite (ATJ) has been determined in air in five different test environments. The stagnation pressures of these environments ranged from 0.035 atm to 15 atm, and the total enthalpies ranged from 2 MJ/kg to 35 MJ/kg. Surface temperatures ranged from 1600° K to 3450° K.

In the higher pressure environments, the mass-loss rates of the glasslike carbons and the pyrolytic graphite were significantly lower than that of the ATJ graphite; however, the pyrolytic graphite tended to delaminate unpredictably. The glasslike carbons tended to develop small pits or craters in their stagnation regions, and wavelike rings, suggestive of surface melting, sometimes formed about their stagnation regions.

The observed mass-loss rates of the several materials studied do not agree well with the diffusion-limited rates predicted by commonly accepted graphite ablation models even though, on the basis of surface temperature and stagnation pressure, the ablation rates should be diffusion limited. In addition, the mass-loss rates of the several materials differ considerably from one another. These facts suggest that the mass-loss rate of carbon is not, at the present test conditions, diffusion limited.

Empirical correlations relating mass-loss rate to surface temperature and stagnation pressure were developed for the several materials studied.

17. Key Words (Suggested by Author(s)) Graphite Ablation Carbon	18. Distribution Statement Unclassified – Unlimited		
19. Security Classif. (of this report) Unclassified	20. Security Classif. (of this page) Unclassified	21. No. of Pages 33	22. Price* $3.00

*For sale by the National Technical Information Service, Springfield, Virginia 22151

ABLATION PERFORMANCE OF GLASSLIKE CARBONS, PYROLYTIC GRAPHITE, AND ARTIFICIAL GRAPHITE IN THE STAGNATION PRESSURE RANGE 0.035 TO 15 ATMOSPHERES

By Howard G. Maahs
Langley Research Center

SUMMARY

The ablation performance of two glasslike carbons (LMSC Glass-like Carbon, Grade 3000, and Vitreous Carbon), one pyrolytic graphite, and one artificial graphite (ATJ) has been determined in air in five different test environments. The stagnation pressures of these environments ranged from 0.035 atm to 15 atm, and the total enthalpies ranged from 2 MJ/kg to 35 MJ/kg. Surface temperatures ranged from approximately 1600° K to 3450° K.

In the higher pressure environments, the mass-loss rates of the glasslike carbons and the pyrolytic graphite were significantly lower than that of the ATJ graphite; however, the pyrolytic graphite tended to delaminate unpredictably. The glasslike carbons tended to develop small pits or craters in their stagnation regions, and wavelike rings, suggestive of surface melting, sometimes formed about their stagnation regions.

The observed mass-loss rates of the several materials studied do not agree well with the diffusion-limited rates predicted by commonly accepted graphite ablation models even though, on the basis of surface temperature and stagnation pressure, the ablation rates should be diffusion limited. In addition, the mass-loss rates of the several materials differ considerably from one another. These facts suggest that the mass-loss rate of carbon is not, at the present test conditions, diffusion limited. A probable explanation for this experimental contradiction to theory, supported by recent experimental data in the literature, is that the oxidation rate of carbon is not as rapid at high temperatures as had been previously accepted.

Empirical correlations relating mass-loss rate to surface temperature and stagnation pressure were developed for the several materials studied.

INTRODUCTION

Glasslike carbons are a relatively new form of carbon, the fabrication of which was first reported in 1961. (See ref. 1.) These carbons exhibit a combination of low density (1.4 g/cm^3 as opposed to about 1.7 g/cm^3 for conventional artificial graphite), impermeability to gases, low thermal conductivity, high strength, and so forth, which is not to be found in other existing forms of carbon. Their appearance is similar to black glass. Physically, they are hard and brittle and are conventionally machined by diamond-grinding techniques. Of particular interest among the reported properties of the glasslike carbons is their resistance to gaseous oxidation. (See refs. 2 to 4.) It has even been indicated (refs. 2 and 3) that at certain temperatures the glasslike carbons are more oxidation resistant than the basal plane of pyrolytic graphite.

The glasslike carbons have the further unique properties that they are homogeneous, isotropic, and, unlike conventional artificial graphites, are single component in composition. Hence, when exposed to a dynamic oxidizing environment, they should not be subject to delamination (as is pyrolytic graphite), nor should they be nearly so susceptible to mechanical erosion as artificial graphite. Accordingly, the glasslike carbons appear to be of interest for potential use in dynamic, high-temperature, aerospace applications.

Pyrolytic graphite is also a material of interest for aerospace applications. This is largely because of its demonstrated high-oxidation resistance relative to conventional artificial graphites (see, for example, refs. 2 and 3), its low across-grain thermal conductivity, and its high across-grain compressive strength.

The present investigation was undertaken to assess the potential of these materials for use in dynamic aerospace environments. The main purpose was to define the pressure and temperature regimes of potential applicability for these materials and also to expose problem areas or undesirable features which might be peculiar to them. So that a meaningful comparison of ablation performance could be made with existing ablation materials, the widely-used artificial graphite, ATJ, was included in all the ablation tests.

The results of an experimental investigation of the ablation performance of two glasslike carbons, one pyrolytic graphite, and, for comparison, one artificial graphite are presented in this report. The parameters selected for assessing ablation performance were total recession for a given test duration, linear stagnation-point mass-loss rate, and steady-state stagnation-point surface temperature. Stagnation-point pressures in the test environments ranged from a low of 0.035 atm to a high of 15 atm, Mach numbers ranged from 2 to 9, and nominal total enthalpies ranged from 2 MJ/kg to 35 MJ/kg. All tests were conducted in air.

SYMBOLS

A,B,C	arbitrary constants
E	Young's modulus, GN/m^2
h	nominal total enthalpy, MJ/kg
k	thermal conductivity, J/cm sec ^oK
Δl_t	change in specimen length resulting from a t-second exposure to the test environment
M	Mach number
$\dot{m}$	linear stagnation-point mass-loss rate, g/cm^2 sec
$\dot{m}_D$	diffusion-limited stagnation-point mass-loss rate for a 0.635-cm nose-radius body, g/cm^2 sec
$\dot{m}_s$	stagnation-point mass-loss rate, $\dot{m}_D$ plus contribution from sublimation, g/cm^2 sec
$p_{t,2}$	stagnation-point pressure, atm (1 atm = 0.1013 MN/m^2)
p_∞	free-stream pressure, atm
q_{cw}	stagnation-point cold-wall heating rate to a 0.635-cm nose-radius hemisphere (cold-wall temperature, 333^o K), W/cm^2
$\overline{q}_{cw}$	nominal value of q_{cw} for a given test condition, W/cm^2
S_T	tensile strength, MN/m^2
T	stagnation-point surface temperature at steady state, ^oK
t	specimen test time, seconds
α	coefficient of thermal expansion, per ^oK

ABBREVIATIONS

ATJ	ATJ graphite
GC	LMSC Glass-like Carbon, Grade 3000
PG	pyrolytic graphite
VC	Vitreous Carbon

EXPERIMENTAL EQUIPMENT AND PROCEDURE

Test Environment

Ablation tests were conducted in five different test environments. These are listed in table I along with the corresponding nominal cold-wall heating rates to a 0.635-cm-radius hemisphere and the facilities in which the particular environments were obtained. Detailed descriptions of these facilities are to be found in references 5 to 8. In all test facilities except the Langley 11-inch ceramic-heated tunnel (CHT), the test gas was heated by passing it through a rotating electric arc. In the CHT, the test gas was heated by passing it through a bed of hot ceramic pebbles. The test gas was always air.

Test-stream stagnation pressures and heating rates in the arc-heated facilities were measured with a calibrated pressure probe and a calibrated Gardon foil asymptotic calorimeter, respectively. For the CHT, test-stream stagnation pressures and enthalpies were obtained from the facility operating conditions by use of figures in reference 8. For all facilities, heating rate was related to enthalpy by the Fay and Riddell equation (ref. 9). The test-stream variables, M and p_∞, listed in table I, were determined for the high-enthalpy arc tunnel at the Langley Research Center (HEAT) and for the Langley 20-inch hypersonic arc-heated tunnel (HAHT) by calculation using reference 10, and for the arc-heated materials jet at the Langley Research Center (AHMJ) and the CHT from charts in reference 11.

Test Specimens

The test specimens employed are shown schematically in figure 1. They consisted of hemisphere-cylinders with 1.270-cm diameters, which were 1.905 cm long and had nose radii of 0.635 cm. The artificial-graphite specimens were machined from a billet of graphite, whereas the glasslike carbons and the pyrolytic graphite, because of fabrication requirements, were fabricated as hemisphere-cylindrical shells mounted on

hemisphere-cylindrical mandrels which were machined from a fine-grained artificial graphite. For ablation testing, the specimens were mounted in a 1.270-cm-diameter, 1.905-cm-long, phenolic-asbestos insulator, which was mounted in a water-cooled holder.

There are a number of different varieties of glasslike carbon. These differ in organic precursor materials (refs. 12 and 13) and fabrication techniques; this information is, however, proprietary. Two different glasslike carbons were selected for study: LMSC Glass-like Carbon, Grade 3000, produced by Lockheed Missiles & Space Company, and Vitreous Carbon, produced by Beckwith Carbon Corporation. According to the Lockheed Missiles & Space Company, the primary precursor of their LMSC Glass-like Carbon, Grade 3000, is a "modified phenolic polymer," with the "3000" designating the maximum heat-treatment temperature in degrees centigrade. No information regarding the primary precursor material of the Vitreous Carbon could be obtained from its manufacturer. However, Yamada (ref. 12) has surmised that the primary precursor of the Vitreous Carbon is a phenol-formaldehyde resin. It is of interest that Yamada also surmised that one precursor of LMSC Glass-like Carbon is naphthalenediol (which is not necessarily contradictory to their stated "modified phenolic polymer"). Selected physical and mechanical properties of these materials as reported by their manufacturers are listed in table II.

The pyrolytic graphite was obtained from Metallurgical Products Department, General Electric Company. It was fabricated from gaseous hydrocarbons by pyrolytic deposition of carbon directly on the artificial-graphite mandrels, with deposition and annealing taking place at about 2370° K. Approximate values of selected properties of this material, obtained from the manufacturer and from reference 14, are listed in table II.

The artificial graphite used as a standard of comparison was ATJ graphite, as commercially supplied by the Union Carbide Corporation. It was selected solely because it is a fine-grained, commercially available artificial graphite with which many investigators have had ablation-testing experience. Selected property data on ATJ graphite obtained from the manufacturer and from reference 15 are included in table II.

The pyrolytic-graphite specimens have a high degree of crystal anisotropy, much as if layers of the material had been wrapped over the curved nose of the hemisphere-cylinder specimens. This layered structure arises as a result of the carbon-deposition process and is not the result of an effort to stack together layers of material. The ATJ graphite is also anisotropic, but not nearly to the extent of the pyrolytic graphite. (The ATJ graphite has an anisotropy ratio of about 1/2, whereas the pyrolytic graphite has an anisotropy ratio of about 1/50. This ratio, a measure of the relative number of crystallite faces lying in a plane parallel to the across-grain direction of the graphite to those lying in the perpendicular plane, that is, in the with-grain direction, was determined for the ATJ graphite by X-ray diffraction using the method of Bacon (ref. 16) and was

estimated for the pyrolytic graphite from thermal expansion coefficients reported by the manufacturer.) All specimens of the ATJ graphite were machined with the across-grain direction parallel to the axis of the specimen, so that during testing the test stream impinged on the specimen in the across-grain direction, that is, in the direction of the lowest thermal conductivity, as with the pyrolytic graphite. Since the glasslike carbons are isotropic, no consideration of specimen orientation was required.

Instrumentation and Data Analysis

Instrumentation for measuring ablation performance consisted of a bench micrometer (direct reading in inches to 0.0001 inch (0.00025 cm)), two high-speed motion-picture cameras, each with a framing rate of 200 pictures per second, and a continuous recording photographic pyrometer, the theory and principle of which is described in reference 17. The parameters selected for assessing ablation performance were total-length change Δl_t resulting from a t-second exposure to the test environment, linear stagnation-point mass-loss rate $\dot{m}$, and steady-state stagnation-point surface temperature T.

Total-length change was obtained from length measurements of the specimen before and after exposure to the test environment. Specimen test time t in each of the different environments is listed in table I. Linear mass-loss rate was determined from the motion-picture-film records of the eroding specimens. Specimen lengths as a function of time were obtained from the film records with the aid of a motion analyzer and were plotted as shown in the sample plot in figure 2. Customarily, specimen length initially increased because of thermal expansion, but soon passed through a maximum, and thereafter continually decreased. Specimen mass-loss rate was determined over the linear part of this length decrease by multiplying the rate of decrease, obtained from a least-squares fit of the data, by the room-temperature density of the material. (The proper high-temperature density to use is uncertain, and, in any event, will change the calculated mass-loss rate by only a few percent.)

Stagnation-point surface temperatures were determined from the motion-picture-film records taken with the photographic pyrometer. For determining these temperatures, the emissivity of the glasslike carbons was assumed to be 0.85 (ref. 18), that of pyrolytic graphite was assumed to be 0.65 (refs. 18 to 20), and that of artificial graphite, 0.94 (ref. 19). A wide spread in emissivity values for pyrolytic graphite has been reported in the literature, with some values even as large as 0.95 (ref. 2). Consequently, the surface temperatures for pyrolytic graphite must be considered as approximate. (Uncertainty in the emissivity results in a temperature uncertainty of about 100° K at high temperatures and of about 50° K at low temperatures.) The specimen surface temperatures were plotted as a function of time as shown in the sample plot (fig. 2) and the representative stagnation-point surface temperature was taken as the steady-state maximum temperature attained during the run. In most test environments, this temperature

was reached during the linear part of the length-time curve, as shown in figure 2. However, a certain amount of subjective judgment was sometimes required for defining this temperature for specimens tested in the highest pressure environment (15 atm).

Typical Test Sequence

With the exception of the tests in the CHT, a typical experimental test sequence proceeded as follows: the electric-arc heater and airflow were started and sufficient time was allowed for the test stream to become fully stabilized. The motion-picture cameras and photographic pyrometer were started, and the test-stream heating rate was measured. The specimen was then inserted into the test stream and allowed to remain for a preset duration. After retraction of the specimen, a final heating-rate measurement was made. Each event in this sequence was executed automatically and controlled by a preset programer.

The test sequence in the CHT was similar, except that the test gas (air) was passed through a bed of hot ceramic pebbles and no heating-rate measurements were made. Total enthalpy was estimated from charts presented in reference 8 relating stream temperature to facility operating conditions, and from this, heating rates were calculated using the Fay and Riddell equation (ref. 9).

RESULTS

Ablation-performance data obtained for the materials studied are presented in table III. These data include total length recession in t seconds Δl_t; linear mass-loss rate $\dot{m}$; and steady-state surface temperature T. Also presented are the cold-wall heating rates for each run q_{cw}, which unavoidably varied slightly from run to run in each nominal test environment.

In several instances in the 0.60-atm, 2.2-atm, and 15-atm test environments, the specimens of glasslike carbon eroded completely through their hemispherical shells exposing their supporting mandrels; thus a measurement of total-length change would be meaningless. Such instances are noted in table III. Also, no data are included in table III for pyrolytic graphite in the 15-atm test environment because of consistent failure of the small mandrels when they were inserted into the test stream. Another phenomenon peculiar to this high-pressure test condition was that the mass-loss-rate data for ATJ graphite could be described by two different rates, each virtually linear. A representative plot depicting this behavior is shown in figure 3. Shortly after an ATJ-graphite specimen was inserted into the test stream at 15 atm, the specimen began to recede at nearly a constant rate, but soon thereafter its recession rate almost tripled. This increase in rate is probably associated with the fact that as the ATJ specimens erode, their originally

hemispherical noses become conical. (See fig. 4.) In a broad sense, therefore, the slower of the two rates may be thought of as associated with the erosion of a hemispherical nose and the development of a conical nose, and the faster of the two rates may be thought of as associated with the erosion of a conical nose. The erosion of ATJ graphite at this high-pressure condition was accompanied by considerable mechanical removal of particulate matter as witnessed from the film records.

The ablation-performance data in table III are also presented in figures 5 to 7. Figure 5 shows the mass-loss rates of the different materials in each of the different environments. For comparison, the diffusion-limited mass-loss rates, $\dot{m}_D$ of a hemisphere-cylinder with a 0.635-cm nose radius, calculated using the diffusion-limited ablation-rate model of Scala (ref. 21), are also shown. Figure 6 shows total-length changes of the same specimens normalized with respect to time. Although such normalization produces a parameter with units of recession rate (cm/sec), it is not a true recession rate in the sense that it is not an instantaneous rate; it may, however, be viewed as an average rate, which rate, of course, is dependent on test duration. Since the time required to establish a constant recession rate varied with test environment, these normalized-length changes are useful primarily for comparing the ablation performance of the different materials for one test environment. Figure 7 shows the surface temperatures of the specimens. All three data figures (figs. 5 to 7) have been drawn with a common abscissa to facilitate comparisons among them, even though this results in some voids in the figures when specific data do not exist.

DISCUSSION

Prior to testing the glasslike carbons, it was suspected that they might be prone to thermal shock since the figure of merit $\left(kS_T/\alpha E\right.$, a measure of thermal shock resistance$\left.\right)$ for LMSC Glass-like Carbon is almost 30 times lower than that for ATJ graphite. (See table II.) However, specimen failure by thermal shock occurred for only one specimen: a part of the nose of a Vitreous Carbon specimen was lost in the 0.60-atm environment shortly after it was inserted into the test stream. The figure of merit for pyrolytic graphite does not have the same significance as that for the other materials studied because the layers in pyrolytic graphite can absorb some thermal stress by shifting slightly with respect to one another. Pyrolytic graphite performed well at pressures below 5.6 atm, with but one indication of thermal shocking: a crack formed in the side of one specimen in the 0.035-atm environment. In the 5.6-atm environment, however, the specimens unpredictably delaminated or otherwise lost chunks of materials from the surface. Although the pyrolytic graphite could not be tested in the 15-atm environment

because of the structural weakness of its mandrels, it is suspected that it would have even less structural integrity in this environment than in the 5.6-atm environment.

One particularly noteworthy result apparent from the present data is that the glasslike carbons are significantly more erosion resistant than ATJ graphite, except at 0.60 atm or below. Even in these low-pressure environments, the glasslike carbons eroded at a rate only slightly faster than ATJ graphite. The largest differences in mass-loss rate occurred at 5.6 atm, where the mass-loss rates of the glasslike carbons were about 1/3 to 1/5 of that of ATJ graphite. This greater erosion resistance at high pressures suggests a definite practical potential for the aerospace application of these materials.

The erosion resistance of the pyrolytic graphite is even greater than that of the glasslike carbons; it is at least as erosion resistant or more so than ATJ graphite at all conditions tested. (See fig. 5.) It has, however, a tendency to delaminate or lose chunks of materials in the higher pressure environments. But, in spite of this, its total mass-loss rate is still less than that for either ATJ graphite or the glasslike carbons. Although the pyrolytic graphite could not be tested in the 15-atm environment, delamination is undoubtedly severe in this environment. Accordingly, the utility of this material appears to be limited to the lower pressure environments. However, since fabrication techniques (which are proprietary information) undoubtedly differ among suppliers, not all pyrolytic graphites will necessarily behave similarly to the one currently under investigation. It would seem unwise, therefore, solely on the basis of the present results, completely to rule out pyrolytic graphite as a material for further consideration for application in higher pressure applications.

The fact that the different materials eroded at different rates is not surprising. For instance, it is well known (see, for example, ref. 22) that differences in crystallite size, crystallite orientation, degree of graphitization, porosity, impurity level, and so forth, can all contribute to differences in oxidation rate. Since the three different types of carbon studied in this investigation differ widely in these properties, they may reasonably be expected to differ in ablation performance. One obvious factor contributing to the high mass-loss rate of ATJ graphite in the higher pressure environments is particle removal, which was particularly apparent in the 15-atm test environment. One factor contributing to the low erosion rate of the pyrolytic graphite is the fact that the crystal-layer faces, instead of the more reactive crystal-layer edges, were exposed to the test stream. The crystal faces of pyrolytic graphite are known to be highly oxidation resistant. (See, for instance, ref. 23.)

Comparisons With Diffusion-Limited Predictions

Diffusion-limited mass-loss rates predicted by the theory of Scala (ref. 21), shown in figure 5, do not agree well with the present mass-loss-rate data.[1] At the three higher pressure conditions, the present experimental data lie considerably below the diffusion-limited predictions, even though the specimen surface temperatures (see fig. 7) are well above those temperatures at which the mass-loss rates are predicted to become limited by diffusion (ref. 21). Of particular note is that these results were obtained in three different facilities and, hence, must be independent of facility. Furthermore, in the one facility in which tests were conducted at two different conditions (that is, the HAHT), one set of data lies close to, but above, the diffusion-limited prediction, whereas the other set lies considerably below. It would appear, therefore, that the test condition itself is the important factor, and not the particular facility in which the test condition was produced.

In the 0.60-atm environment, the mass-loss rates of all the materials tested lie above the predicted diffusion-limited rate. Because the specimen surface temperatures at this condition were on the order of 3400° K, at which temperature the vapor pressure of carbon has been variously reported to lie between a low of 0.005 atm and a high of 0.5 atm (see, for instance, ref. 26), it is likely that sublimation is contributing to the total mass-loss rates. An estimation of the mass-loss rate including sublimation $\dot{m}_S$ can be calculated from an expression given in reference 27 relating $\dot{m}_S$ to $\dot{m}_D$. Such mass-loss rates $\dot{m}_S$ are indicated in figure 5, where, in order to give an upper bound, they have been based on the predicted $\dot{m}_D$ of Scala for a 0.635-cm nose-radius body. Values of $\dot{m}_S$ based on an $\dot{m}_D$ calculated using effective nose radius are, of course, somewhat lower, but, for the sake of clarity, are not shown in the figure.

[1]The diffusion limits shown in figure 5 are for a 0.635-cm nose-radius body – the initial geometry of the specimens. However, by using the method of reference 24 and photographs of the specimens, such as those in figure 8, effective nose radii can be calculated enabling adjustment of these diffusion limits for the actual shapes attained by the specimens during the tests. With the exception of ATJ graphite tested at 15 atm, these calculations tend to reduce the diffusion limit somewhat, with the adjusted values being indicated by the horizontal solid lines in figure 5. The adjusted diffusion limit for ATJ at 15 atm is approximate because the specimen became conical during the test; however, this limit is of little significance since a large portion of the total mass-loss rate was due to particle removal in addition to oxidative removal.

It is recognized that other diffusion-limit theories predict somewhat different values than the theory of Scala. For instance, the diffusion limit of Miller and Sutton (ref. 25) is 0.86 times the diffusion limit of Scala. Such differences in theories do not affect the qualitative nature of the present discussion.

For the lowest pressure environment (0.035 atm), the predicted diffusion-limited rate agrees more closely with the experimentally observed rates. It would be imprudent, however, to construe these few points of agreement as proof that these erosion rates are diffusion limited, particularly in view of the other experimental data presented.

A second and even more forceful argument can be advanced to demonstrate that the mass-loss rate of carbon is not diffusion limited at the conditions of the present tests. According to the concept of a diffusion-limited rate, the mass-loss rates for all materials which are diffusion limited must be the same. But figure 5 clearly shows that the mass-loss rates of the glasslike carbons, pyrolytic graphite, and ATJ graphite differ appreciably. Accordingly, the conclusion seems inescapable that the mass-loss rate of carbon is not diffusion limited at the present conditions. It also seems obvious that the actual rate is dependent on the carbon type and, hence, on chemical kinetics.

This conclusion confirms a similar conclusion reached in an earlier paper (ref. 28), in which several different artificial graphites were studied at 5.6 atm, but over the temperature range 1750° K to 2300° K. In this earlier work, a definite dependence of reaction rate on temperature was observed.

A brief discussion of one probable explanation for these experimental contradictions to current diffusion-limited ablation-rate models might be in order. First of all, it must be appreciated that even though the concept that the rate of a reaction can be controlled by the diffusion of reactant to the reacting surface lies on firm theoretical ground, many of the requisite data inputs to the theory applicable to the oxidation of carbon must be calculated, estimated, or even assumed. For example, the particular chemical species produced by the reaction of air with carbon at these conditions is not experimentally certain, the diffusion rates of the species through the boundary layer (and even the composition of the boundary layer) are not experimentally known, and the chemical kinetic mechanism and rate constants of the air-carbon reaction are not certain, particularly at high temperatures. The possibility of particle removal further complicates the description. Probably the most restrictive of these inputs to the theory is the uncertainty concerning the mechanism and reaction rate. Scala (ref. 21), in developing his diffusion-limited model, drew upon literature data for reaction rates, all of which were obtained below 1370° K. These data were approximated by an Arrhenius equation, and this equation was then extrapolated by a straight line to cross an independently calculated diffusion-limited-rate curve. Implicit in such an extrapolation is the assumption that the activation energy of the chemical reaction is a constant. Although this is frequently a convenient assumption to make in the absence of data to the contrary, it is without theoretical justification. (See, for instance, ref. 29.) In fact, experimental data on the carbon-oxygen reaction at high temperatures indicating that such an extrapolation is invalid have been published by several authors (refs. 2 and 29 to 34); these data show a pronounced curvature on an

Arrhenius plot, even to the extent of producing a maximum in the rate curve. This curvature could very well result in the reaction-rate curve never intersecting the diffusion-limited-rate curve; that is, the mass-loss rate of carbon could be controlled by chemical kinetics even at very high temperatures.

One other factor which may partially account for the deviation of the present data from Scala's diffusion-limited prediction is that Scala drew his kinetic data from literature sources in which different types of carbons from those studied in the present investigation were studied. But it is well known that the type of carbon can have a remarkable effect on chemical reaction rate. (See, for instance, refs. 2, 30, and 33.) Therefore, the chemical oxidation rates of the carbons used by Scala in developing his ablation-rate model could differ considerably from those of the present materials. To investigate in detail these foregoing points would require a comprehensive study in itself; however, because a commonly accepted model for the high-temperature ablation of graphite could be markedly affected, such a study seems to be thoroughly justified.

Surface Features After Test

A photograph of selected specimens from the present tests is shown in figure 8. This photograph depicts the four different materials before testing, after testing for 60 seconds at 0.035 atm, and after testing for 30 seconds at 5.6 atm. In the 0.035-atm environment, all four materials essentially retained their hemispherical shape, and, in addition, the pyrolytic graphite and the LMSC Glass-like Carbon became highly polished. The Vitreous Carbon became slightly dull in the stagnation region, which region, on close examination, revealed many very small pocks or pits. Close examination of the pyrolytic graphite revealed that several layers of material had eroded through in the stagnation region, as evidenced by a series of concentric rings about the stagnation region consisting of the edges of layers.

In the 5.6-atm environment, all materials became blunted. Also, both glasslike carbons became dull in appearance. The stagnation region of the LMSC Glass-like Carbon revealed small, but nevertheless obvious, pits or craters, while the Vitreous Carbon revealed considerably deeper craters, which imparted a very rough texture to the surface. The oxidation pitting of glasslike carbons is described in reference 35, where, although the phenomenon is admittedly not thoroughly understood, it is surmised that such pitting occurs at sites of catalytic impurities in the material. Also in the 5.6-atm environment, the pyrolytic graphite specimens lost sizable pieces of material from their shoulder regions and from well down on their sides, much as if blisters had formed and burst, exposing material underneath. In one test, a shell consisting of the outer layers of the specimen was blown completely off. Oxidation pitting of pyrolytic graphite is also described in reference 35, but no such pits were observed in the present material.

Several of the glasslike carbons tested in the higher pressure environments developed a small, wavelike, protruding ring encircling the stagnation region, suggestive of melting or plastic deformation. (See fig. 9.) Outside of this ring was a duller surface containing many small pocks or pits. These ringlike surface features were most obvious in the 2.2-atm test environment, but they were also observed in several specimens tested in the 5.6-atm environment. They were not observed in the 15-atm environment; however, in all these tests, the glasslike carbon shells were eaten through to their mandrels.

What is responsible for this surface phenomenon is uncertain. According to the phase diagram of carbon (see, for instance, ref. 36), no melt phase should occur for carbon at pressures below 100 atm and temperatures below 4000° K. Glasslike carbon, however, is not a true equilibrium phase of carbon and, hence, does not appear on the phase diagram. For this reason and also because property data are lacking at high temperatures at pressures other than 1 atm, it could be that the glasslike carbons have undergone plastic deformation by the aerodynamic shear forces associated with the high pressures and temperatures of the present environments. In partial support of this, the present wave-ring patterns, shown in figure 9, are reminiscent of the patterns observed on tektites and on glass models ablated by aerodynamic heating. (See refs. 37 and 38.) However, other causes could also produce these wave-like rings. For instance, they could be caused by unusual erosion patterns peculiar to the interaction of these materials with certain dynamic air environments. (See, for instance, ref. 39.) In any event, this phenomenon may be of sufficient interest or importance to warrant future investigation, particularly in the event that the glasslike carbons are considered for use as ablation materials in environments where this phenomenon is known or suspected to occur.

Correlations of Mass-Loss-Rate Data

In the present investigation, mass-loss-rate data were obtained on four different materials in five widely differing environments; however, because of facility limitations, it was not possible to vary pressure, enthalpy, or velocity independently over a meaningful range. It was not possible, therefore, to experimentally determine the individual effects of these important variables. Accordingly, it would be difficult from these raw data to estimate the performance of these materials in environments somewhat different from those of the present investigation. To facilitate making such engineering-performance estimates, simple empirical correlations were developed from the data for each material studied.

The form of correlating equation was

$$\dot{m} = Ae^{B/T}\left(p_{t,2}\right)^{C}$$

where A, B, and C are constants determined from the data. This form of equation is purely empirical and is not intended to describe the fundamental chemical and physical mechanisms of erosion. Values of the constants A, B, and C are presented for the various materials in table IV. Two separate correlations for the ATJ graphite are shown: one which correlates the data with the slower rate in the 15-atm test environment and one which correlates the data with the faster rate, although it is recognized that the slower rate represents a transient condition. The choice of which two of these correlations to use depends, of course, on the particular situation and environmental conditions with which the user is concerned. In spite of the empirical nature of these correlations, it is believed that they may be useful for making preliminary engineering estimates of the mass-loss rates of the glasslike carbons, pyrolytic graphite, and ATJ graphite in the pressure and temperature ranges of the present data, that is, in the pressure range 0.035 atm to 15 atm, and the temperature range 1600° K to 3450° K. These correlations should not be used outside these ranges. For visual inspection of how well the correlations predict the present data, plots of predicted mass-loss rate as a function of observed mass-loss rate are shown in figures 10(a) to 10(e).

CONCLUSIONS

The ablation performance of two glasslike carbons (LSMC Glass-like Carbon, Grade 3000, and Vitreous Carbon), one pyrolytic graphite, and one artificial graphite (ATJ) has been measured in five different test environments. As a result of these measurements and an analysis of the data, the following conclusions are drawn:

1. The glasslike carbons are not significantly more prone to thermal shock than ATJ graphite in the present test environments.

2. The pyrolytic graphite tested has a tendency to delaminate unpredictably or lose chunks of material from its surface in the higher pressure environments.

3. In test environments at pressures greater than 0.60 atm, the glasslike carbons and the pyrolytic graphite are significantly more erosion resistant than the ATJ graphite. In test environments at pressures of 0.60 atm and below, the glasslike carbons erode at a rate slightly higher than the ATJ graphite, but still, the pyrolytic graphite is at least as erosion resistant or more so than the ATJ graphite.

4. The glasslike carbons sometimes developed small pits or craters in the stagnation region. This pitting was more pronounced in the higher pressure environments. No such pitting occurred in the pyrolytic graphite.

5. In the higher pressure environments, the glasslike carbons tended to develop a wavelike ring encircling the stagnation region. This ring is suggestive of melting or plastic deformation under high-shear aerodynamic flow. The pyrolytic graphite showed

no such rings. In the lowest pressure environments, the LMSC Glass-like Carbon and the pyrolytic graphite remained smooth and even developed a polished appearance.

6. Although the mass-loss rate of carbon at the present test conditions is predicted by currently accepted graphite ablation models to be diffusion limited, the present mass-loss-rate data do not confirm these predictions. Instead, they appear to be dependent on carbon type, and hence, on chemical kinetics.

7. Empirical correlations were developed for the materials studied relating mass-loss rate to surface temperature and stagnation pressure. These correlations may be useful for estimating mass-loss rates in environments somewhat different from those considered in this investigation but should be used only within the pressure and temperature ranges of the present investigation.

8. The overall ablation performance of the glasslike carbons, particularly at the higher pressures, suggests a definite practical potential for the aerospace application of these materials.

Langley Research Center,
National Aeronautics and Space Administration,
Hampton, Va., October 13, 1970.

REFERENCES

1. Tsuzuku, T.; and Kobayashi, H.: Internal Friction of Carbon Materials. Proceedings of the Fifth Conference on Carbon, Vol. 2, Macmillan Co., 1963, pp. 539-543.

2. Lewis, J. C.; Floyd, I. J.; and Cowlard, F. C.: A Comparative Study of the Gaseous Oxidation of Vitreous Carbon and Various Graphites at 1500-3000°K. Paper presented at the Eighth Biennial Conference on Carbon (Buffalo, N.Y.), June 1967.

3. Bradshaw, W.: Oxidation of Graphite and Various Types of Carbon. Summary of the Seventh Refractory Composites Working Group Meeting, Vol. 1, RTD-TDR-63-4131, U.S. Air Force, Nov. 1963, pp. 286-295. (Available from DDC as AD 601 264.)

4. Cowlard, F. C.; and Lewis, J. C.: Vitreous Carbon – A New Form of Carbon. J. Mater. Sci., vol. 2, no. 6, Nov. 1967, pp. 507-512.

5. Wells, William L.: Description of the High-Enthalpy Arc Tunnel at the Langley Research Center Including Test-Stream Conditions at Selected Operating Points. NASA TN D-5295, 1969.

6. Midden, Raymond E.; and Cocke, Bennie W., Jr.: Description and Initial Calibration of the Langley 20-Inch Hypersonic Arc-Heated Tunnel. NASA TN D-4653, 1968.

7. Mayo, Robert F.; Wells, William L.; and Wallio, Milton A.: A Magnetically Rotated Electric Arc Air Heater Employing a Strong Magnetic Field and Copper Electrodes. NASA TN D-2032, 1963.

8. Sutton, Kenneth: Description and Operating Parameters of a Mach 2 Nozzle System for the Langley 11-Inch Ceramic-Heated Tunnel. NASA TN D-4750, 1968.

9. Fay, J. A.; and Riddell, F. R.: Theory of Stagnation Point Heat Transfer in Dissociated Air. J. Aeronaut. Sci., vol. 25, no. 2, Feb. 1958, pp. 73-85, 121.

10. Lordi, J. A.; Mates, R. E.; and Moselle, J. R.: Computer Program for the Numerical Solution of Nonequilibrium Expansions of Reacting Gas Mixtures. Rep. No. AD-1689-A-6 (Contract No. NASr-109), Cornell Aeron. Lab., Inc., Oct. 1965.

11. Ames Research Staff: Equations, Tables, and Charts for Compressible Flow. NACA Rep. 1135, 1953. (Supersedes NACA TN 1428.)

12. Yamada, Shigehiko: A Review of Glasslike Carbons. DCIC-68-2 (Contract F33615-67-C-1472), Battelle Memorial Inst. (Available from DDC as AD 668 465.)

13. Yamada, S.; Sato, H.; and Ishii, T.: Properties and Use of Glassy Carbon. Lockheed Missiles & Space Co. Transl. (From Tanso, vol. 2, no. 2, 1964, pp. 253-260.)

14. Anon.: Advanced Materials Technology. Hardware for Cryogenic to 6000 F and Above Environments. Super-Temp Corp.

15. Anon.: The Industrial Graphite Engineering Handbook. Union Carbide Corp., c.1964.

16. Bacon, G. E.: A Method for Determining the Degree of Orientation of Graphite. J. Appl. Chem. (London), vol. 6, 1956, pp. 477-481.

17. Exton, Reginald J.: Theory and Operation of a Variable Exposure Photographic Pyrometer Over the Temperature Range 1800° to 3600° F (1255° to 2255° K). NASA TN D-2660, 1965.

18. Autio, G. W.; and Scala, E.: The Effect of Anisotropy on Emissivity. Carbon, vol. 6, no. 1, Feb. 1968, pp. 41-54.

19. Wilson, R. Gale; and Spitzer, Cary R.: Visible and Near-Infrared Emittance of Ablation Chars and Carbon. AIAA J., vol. 6, no. 4, Apr. 1968, pp. 665-671.

20. Autio, G. W.; and Scala, E.: The Normal Spectral Emissivity of Isotropic and Anisotropic Materials. Carbon, vol. 4, no. 1, May 1966, pp. 13-28.

21. Scala, Sinclaire M.: The Ablation of Graphite in Dissociated Air. Pt. I: Theory. R62SD72, Missile and Space Div., Gen. Elec. Co., Sept. 1962.

22. Walker, P. L., Jr.; Rusinko, Frank, Jr.; and Austin, D. G.: Gas Reactions of Carbon. Advances in Catalysis and Related Subjects, Vol. XI, D. D. Eley, P. W. Selwood, and Paul B. Weisz, eds., Academic Press, Inc., 1959, pp. 133-221.

23. Horton, W. S.: Oxidation Kinetics of Pyrolytic Graphite. Proceedings of the Fifth Conference on Carbon, Vol. 2, Macmillan Co., 1963, pp. 233-241.

24. Zoby, Ernest V.; and Sullivan, Edward M.: Effects of Corner Radius on Stagnation-Point Velocity Gradients on Blunt Axisymmetric Bodies. NASA TM X-1067, 1965.

25. Miller, Irvin M.; and Sutton, Kenneth: An Experimental Study of the Oxidation of Graphite in High-Temperature Supersonic and Hypersonic Environments. NASA TN D-3444, 1966.

26. Dolton, T. A.; Maurer, R. E.; and Goldstein, H. E.: Thermodynamic Performance of Carbon in Hyperthermal Environments. AIAA Pap. No. 68-754, June 1968.

27. Scala, Sinclaire M.; and Gilbert, Leon M.: Sublimation of Graphite at Hypersonic Speeds. AIAA J., vol. 3, no. 9, Sept. 1965, pp. 1635-1644.

28. Maahs, Howard G.: Effects of Natural Chemical Impurities and Crystallite Orientation on the Erosion Behavior of Artificial Graphite. NASA TN D-6023, 1970.

29. Ong, J. N., Jr.: On the Kinetics of Oxidation of Graphite. Carbon, vol. 2, no. 3, Dec. 1964, pp. 281-297.

30. Nagle, J.; and Strickland-Constable, R. F.: Oxidation of Carbon Between 1000-2000°C. Proceedings of the Fifth Conference on Carbon. Vol. 1, Pergamon Press, Inc., 1962, pp. 154-164.

31. Walls, J. R.; and Strickland-Constable, R. F.: Oxidation of Carbon Between 1000-2400°C. Carbon, vol. 1, no. 3, Apr. 1964, pp. 333-338.

32. Rosner, D. E.; and Allendorf, H. D.: High Temperature Oxidation of Carbon by Atomic Oxygen. Carbon, vol. 3, no. 2, Oct. 1965, pp. 153-156.

33. Rosner, Daniel E.; and Allendorf, H. Donald: Comparative Studies of the Attack of Pyrolytic and Isotropic Graphite by Atomic and Molecular Oxygen at High Temperatures. AIAA J., vol. 6, no. 4, Apr. 1968, pp. 650-654.

34. Blyholder, G.; Binford, J. S.; and Eyring, H.: A Kinetic Theory for the Oxidation of Carbonized Filaments. J. Phys. Chem., vol. 62, no. 3, Mar. 1958, pp. 263-267.

35. Blackman, L. C. F.: Oxidation Pitting of Pyrolytic Graphite and Vitreous Carbon. Carbon, vol. 5, no. 2, Apr. 1967, pp. 196-197.

36. Nightingale, R. E.; Yoshikawa, H. H.; and Losty, H. H. W.: Physical Properties. Nuclear Graphite, R. E. Nightingale, ed., Academic Press, Inc., 1962, pp. 117-194.

37. Chapman, Dean R.; and Larson, Howard K.: The Lunar Origin of Tektites. NASA TN D-1556, 1963.

38. Chapman, Dean R.; Larson, Howard K.; and Anderson, Lewis A.: Aerodynamic Evidence Pertaining to the Entry of Tektites Into the Earth's Atmosphere. NASA TR R-134, 1962.

39. Larson, H. K.; and Mateer, G. G.: Cross-Hatching – A Coupling of Gas Dynamics With the Ablation Process. AIAA Pap. No. 68-670, June 1968.

TABLE I.- TEST ENVIRONMENTS AND HEATING RATES

Stagnation pressure, $p_{t,2}$, atm	Mach number, M	Nominal total enthalpy, h, MJ/kg	Nominal heating rate, $\bar{q}_{cw}$, W/cm2	Free-stream pressure, p_∞, atm	Test time, t, sec	Facility	Reference
0.035	9.0	34.9	760	0.0002	60	HEAT	5
.60	4.3	23.0	2066	.023	45	HAHT	6
2.2	4.0	4.63	757	.13	60	HAHT	6
5.6	2.5	2.36	562	.66	30	AHMJ	7
15	2.1	2.55	1011	2.43	20	CHT	8

TABLE II.- APPROXIMATE MATERIAL PROPERTIES

Property	LMSC Glass-like Carbon	Vitreous Carbon	Pyrolytic graphite[a]	ATJ graphite[a]
Density,[b] g/cm^3	1.41	1.49	2.15	1.72
Young's modulus, GN/m^2 (psi)	20.7 (3.0×10^6)	24.1 (3.5×10^6)	[c]10.3 (1.5×10^6)	7.6 (1.1×10^6)
Tensile strength, MN/m^2 (psi)	87.6 (12.7×10^3)	----------	10.3 (1.5×10^3)	23.4 (3.4×10^3)
Compressive strength, MN/m^2 (psi)	597 (86.6×10^3)	689 (100×10^3)	469 (68×10^3)	60.7 (8.8×10^3)
Flexural strength, MN/m^2 (psi)	90.3 (13.1×10^3)	152 (22.0×10^3)	10.3 (1.5×10^3)	24.8 (3.6×10^3)
Thermal conductivity, J/cm sec ^oK	0.033	0.063	0.017	0.92
Thermal expansion, per ^oK	5.0×10^{-6}	3.0×10^{-6}	19.4×10^{-6}	3.5×10^{-6}
Permeability (helium), cm^2/sec	10^{-7} to 10^{-9}	$<2.5 \times 10^{-12}$	----------	[d]5.9
Figure of merit,[e] $kS_T/\alpha E$, J/cm sec	27.9	----------	0.88	812

[a]Values for across-grain properties.

[b]Determined by author.

[c]Estimated from reference 14.

[d]Calculated from data presented in reference 15.

[e]Calculated from data in this table.

TABLE III.- ABLATION PERFORMANCE

Material	Heating rate, q_{cw}, W/cm^2	Total recession in t sec, Δl_t, cm	Mass-loss rate, $\dot{m}$, g/cm^2 sec	Surface temperature, T, ^{o}K
$p_{t,2}$ = 0.035 atm; h = 34.9 MJ/kg; t = 60 sec; facility, HEAT				
LMSC Glass-like Carbon	781	0.1793	0.005 098	2578
	764	.1791	.004 967	----
	764	.1816	.004 129	2578
Vitreous Carbon	758	.1671	.003 851	2600
	760	.1661	.004 293	2606
	772	.1679	.004 197	2572
Pyrolytic graphite	750	.1199	.004 991	2339
	734	.1092	.003 639	2478
	780	.1140	.003 914	2422
ATJ graphite	769	.1598	.004 264	2494
	760	.1669	.003 594	2483
	750	.1570	.004 181	2478
$p_{t,2}$ = 0.60 atm; h = 23.0 MJ/kg; t = 45 sec; facility, HAHT				
LMSC Glass-like Carbon	2140	(a)	0.023 92	3450
	1980	(a)	.021 59	3339
	2095	(a)	.022 19	3422
Vitreous Carbon	2075	(a)	.020 26	3356
	2030	(a)	.022 22	3339
Pyrolytic graphite	1970	.4191	.017 00	3172
	2050	.4204	.018 40	3161
	2155	.4224	.018 88	3228
ATJ graphite	2110	.5441	.020 73	3422
	2130	.5339	.020 17	3450
	1980	.5136	.019 25	3256
$p_{t,2}$ = 2.2 atm; h = 4.63 MJ/kg; t = 60 sec; facility, HAHT				
LMSC Glass-like Carbon	762	(a)	0.008 544	1961
	732	(a)	.008 059	1978
	758	(a)	.008 404	1978
Vitreous Carbon	766	0.2931	.007 360	1889
	758	(a)	.008 721	2011
	796	(a)	.008 171	2042
Pyrolytic graphite	789	.0566	.001 867	1844
	720	.0554	.002 297	1978
	744	.0625	.001 935	1894
ATJ graphite	765	(b)	.015 88	1983
	755	.5398	--------	2061
	822	.5204	.015 32	2075
	701	.4829	.016 77	2078
$p_{t,2}$ = 5.6 atm; h = 2.36 MJ/kg; t = 30 sec; facility, AHMJ				
LMSC Glass-like Carbon	560	0.1013	0.005 453	1667
	545	.0993	.005 448	1600
	525	.1346	.008 249	1689
	570	.1897	.011 70	1783
Vitreous Carbon	580	.2268	.012 41	1733
	590	.1969	.010 46	1744
	571	.2083	.010 88	1756
	574	.2075	.010 09	1783
Pyrolytic graphite	564	.0904	.003 094	1839
	548	.1105	.009 448	1672
	545	.0622	.004 336	1744
ATJ graphite	567	.3828	.028 75	2056
	554	.4333	.030 85	2089
	590	.4615	.030 12	2111
$p_{t,2}$ = 15 atm; h = 2.55 MJ/kg; t = 20 sec; facility, CHT[c]				
LMSC Glass-like Carbon	[d]1011	(e)	0.043 24	2422
	1011	(a)	.041 11	2328
	1011	(a)	.038 38	2394
Vitreous Carbon	1011	(a)	.042 37	2311
	1011	(e)	.039 56	2406
	1011	(a)	.043 13	2422
ATJ graphite	1011	1.0269	[f]0.056 40; 0.127 0	2644
	1011	1.0112	[f].058 02; .118 2	2533
	1011	1.1069	[f].050 16; .130 5	2561

[a]Specimen eroded through to the mandrel.

[b]Test time was only 49 seconds because of an arc blowout in the facility.

[c]The pyrolytic graphite could not be tested at this condition because of consistent failure of the mandrels.

[d]Heating rates were estimated from facility operating conditions.

[e]Specimen was lost during retraction from stream.

[f]The first figure is the rate early in the test, and the second is the rate later in the test.

TABLE IV.- MASS-LOSS-RATE CORRELATIONS

$$\left[\dot{m} = Ae^{B/T}\left(p_{t,2}\right)^{C}\right]$$

Material	A	B	C	Average residual, percent	Maximum residual, percent	Equation
LMSC Glass-like Carbon	0.227	-7045	0.458	12.3	37.7	1
Vitreous Carbon	.176	-6360	.453	13.4	36.6	2
Pyrolytic graphite	.292	-8505	.231	40.8	106.6	3
ATJ graphite [a]	.059	-3050	.411	8.1	22.9	4
ATJ graphite [b]	.217	-6745	.761	18.6	73.4	5

[a]Using the slower rate in the 15-atm environment.

[b]Using the faster rate in the 15-atm environment.

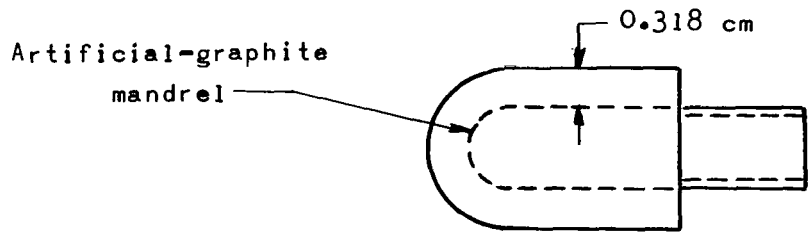

(a) Glasslike carbons.

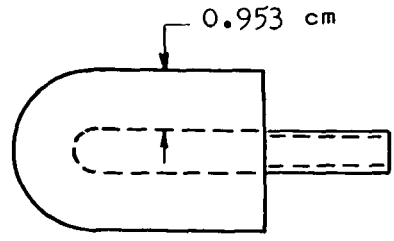

(b) Pyrolytic graphite.

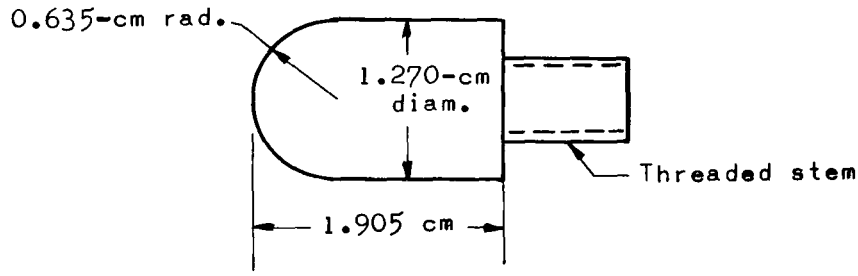

(c) Artificial graphite (ATJ). (Specimen dimensions are typical.)

Figure 1.- Schematic diagram of test specimens.

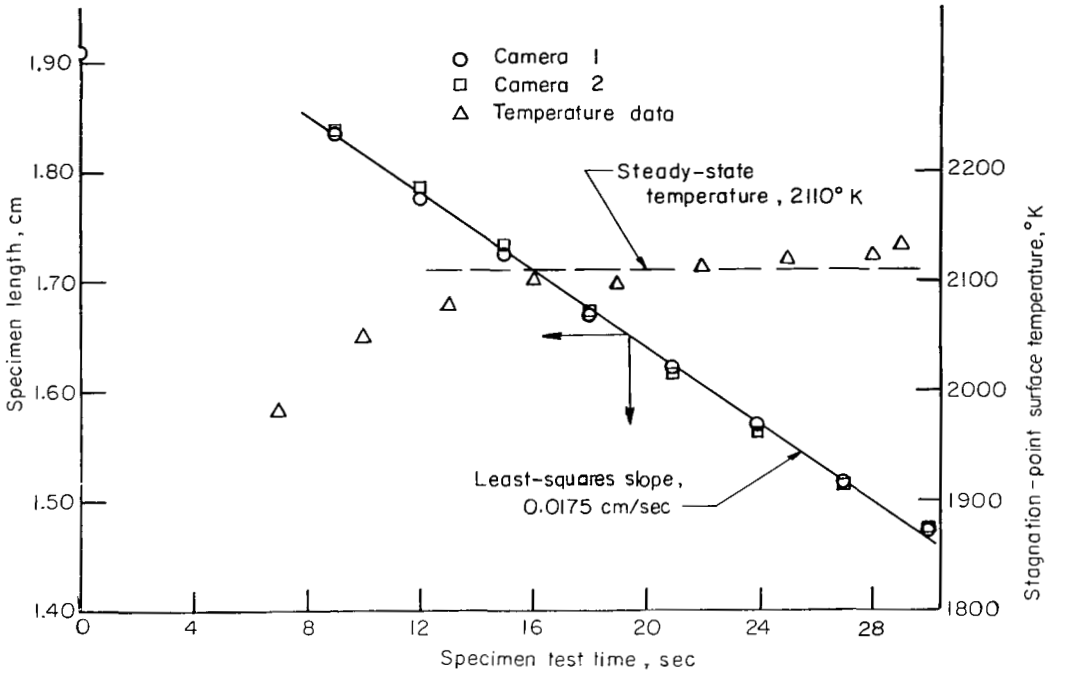

Figure 2.- Sample plot of specimen length and surface temperature as a function of time. (ATJ graphite, 5.6-atm test environment.)

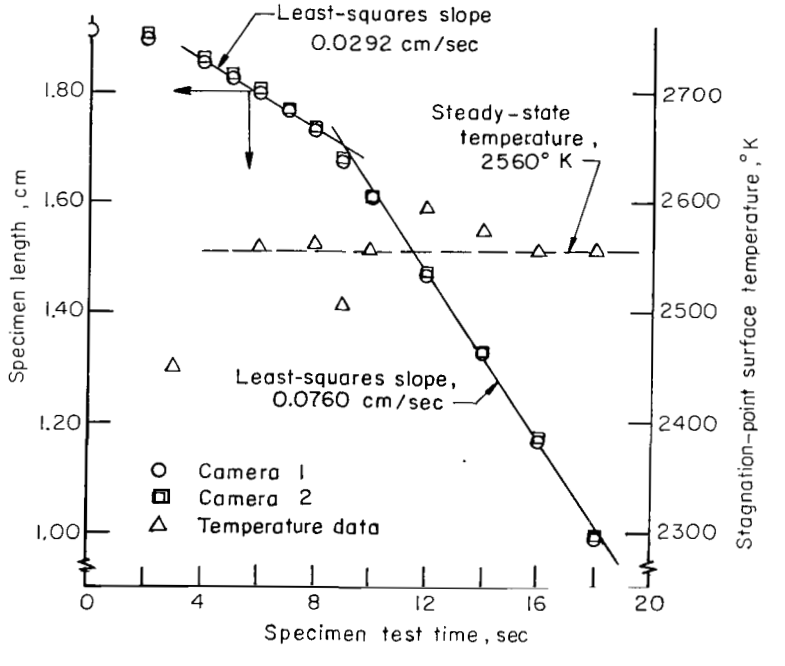

Figure 3.- Representative plot depicting the two mass-loss rates for ATJ graphite in the 15-atm test environment.

L-70-4783

Figure 4.- Conical shape of ATJ-graphite specimen after test in 15-atm test environment.

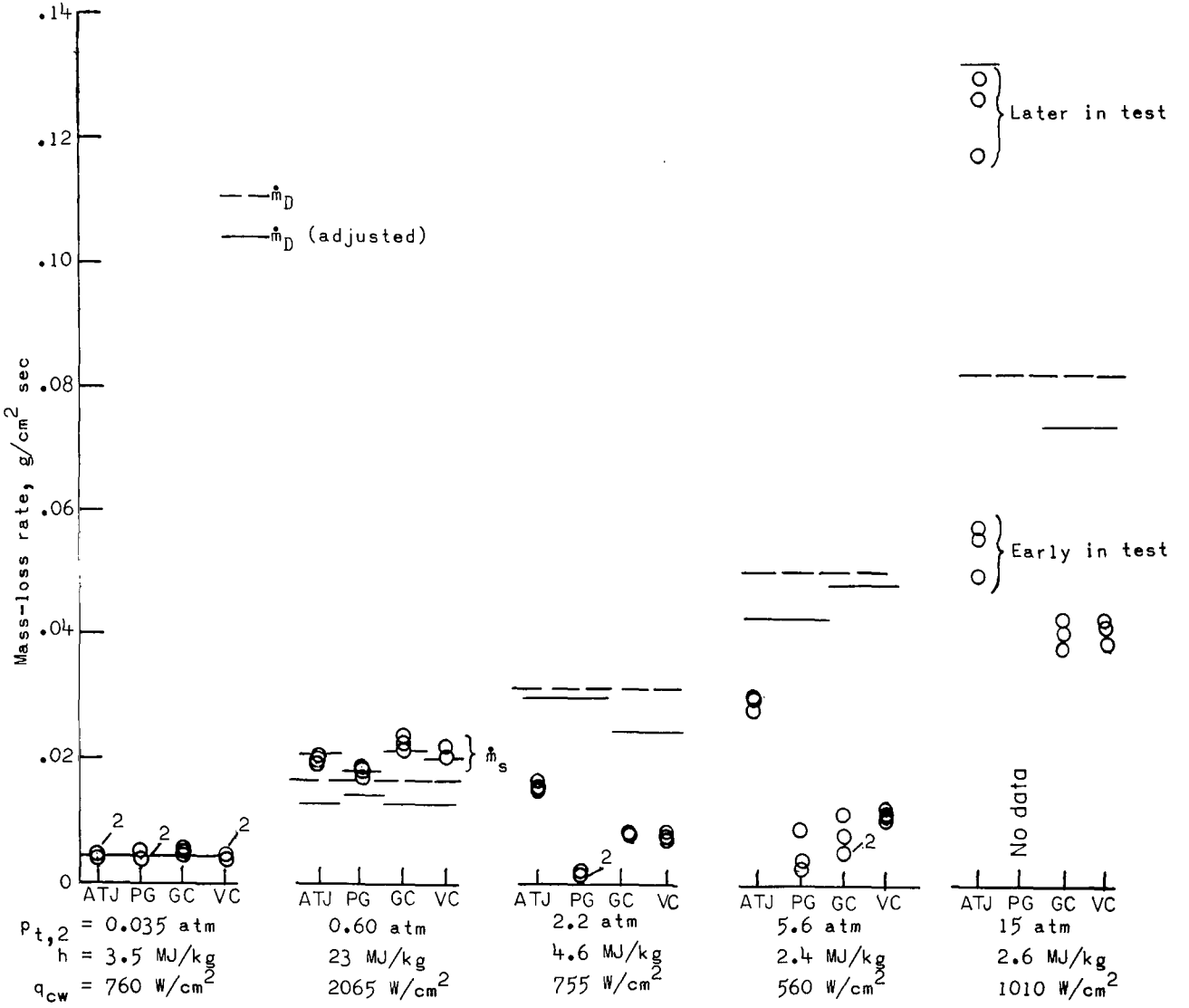

Figure 5.- Mass-loss rates of glasslike carbons, pyrolytic graphite, and ATJ graphite in various environments.

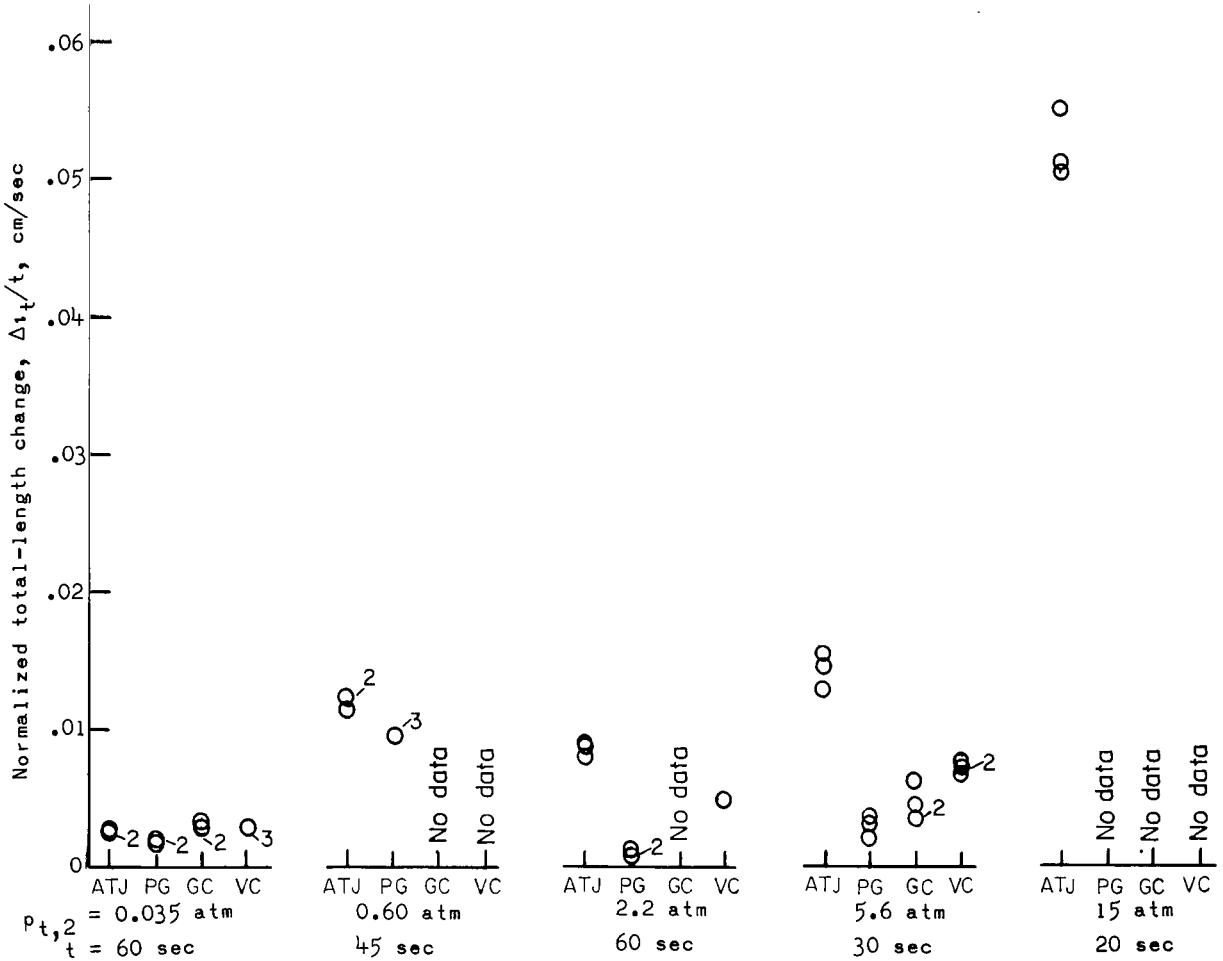

Figure 6.- Normalized total-length change of glasslike carbons, pyrolytic graphite, and ATJ graphite in various environments.

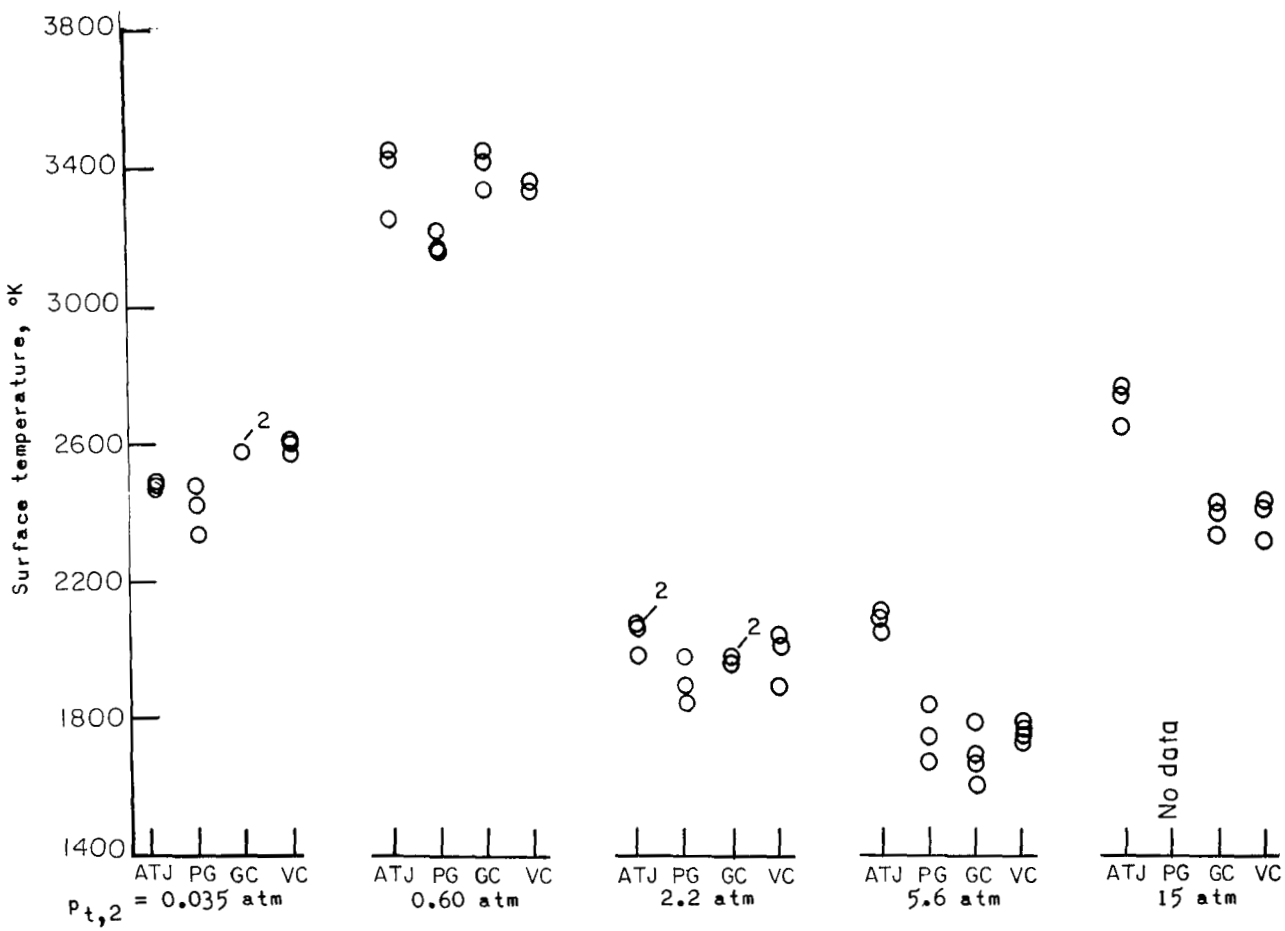

Figure 7.- Surface temperature of glasslike carbons, pyrolytic graphite, and ATJ graphite in various environments.

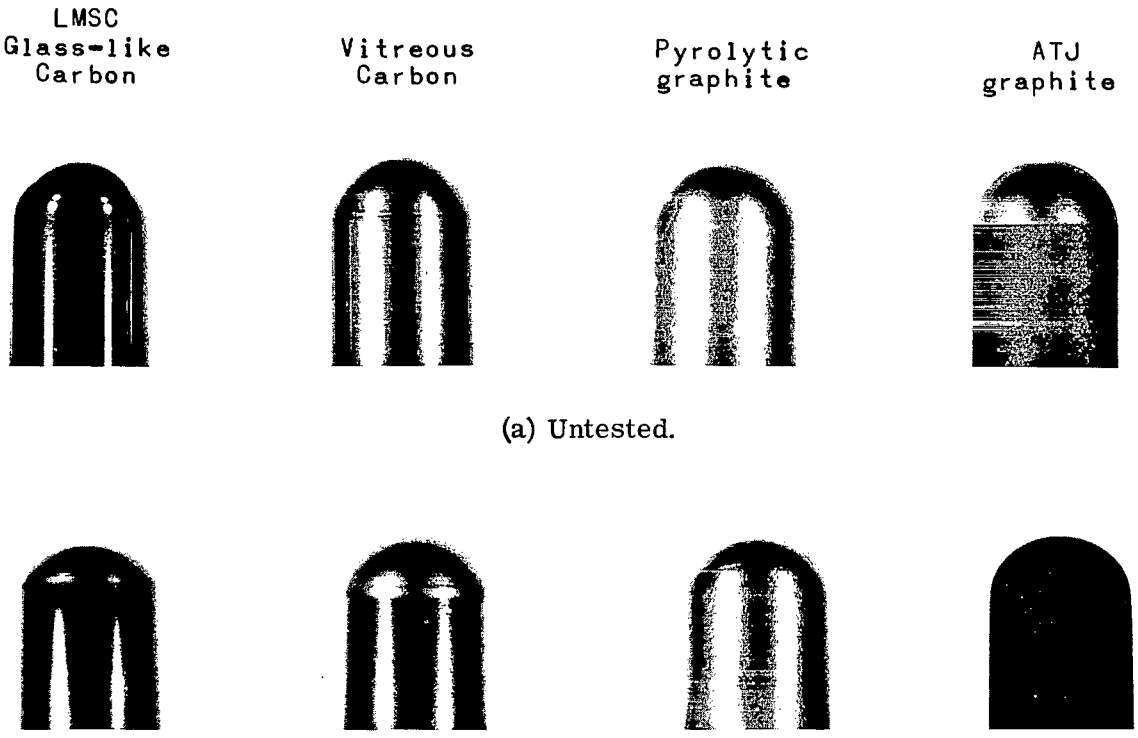

(a) Untested.

(b) Tested in the 0.035-atm environment for 60 seconds.

L-70-4784

(c) Tested in the 5.6-atm environment for 30 seconds.

Figure 8.- Photograph of selected specimens.

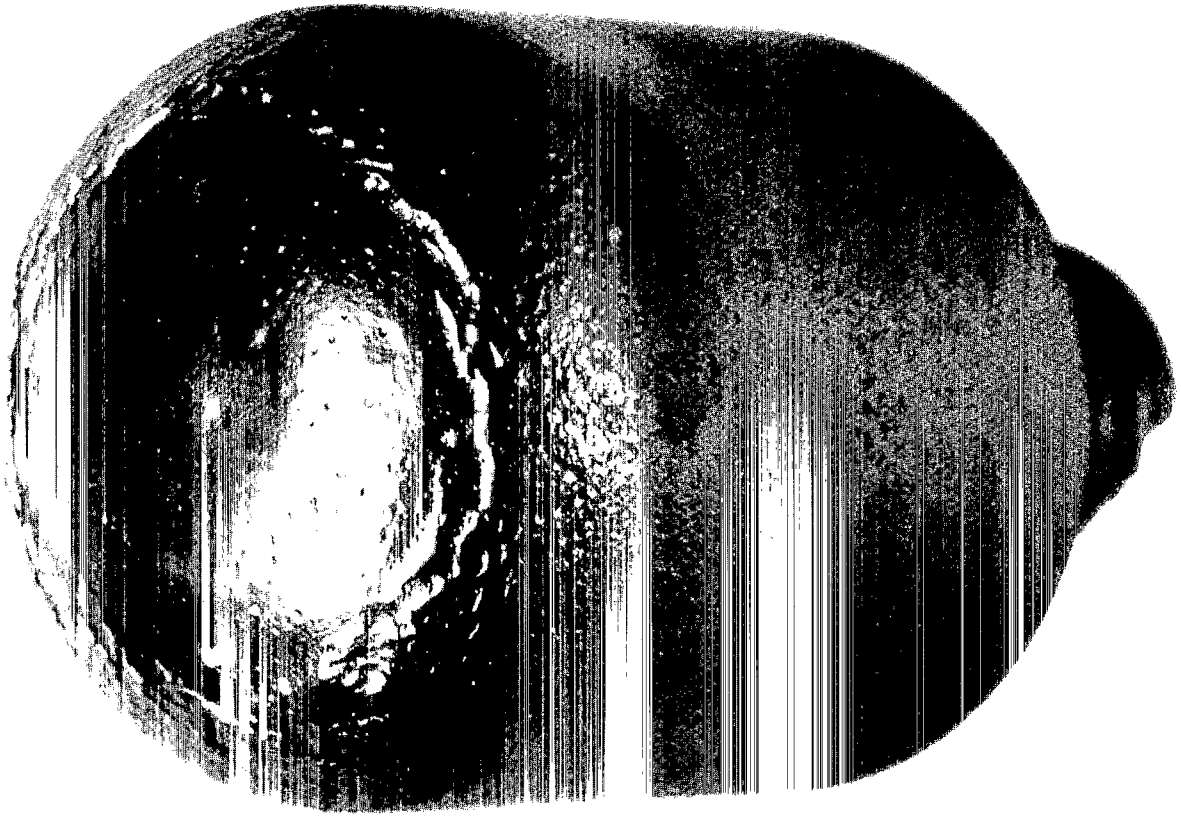

L-70-4785

Figure 9.- Vitreous Carbon specimen showing wavelike ring encircling the stagnation region.

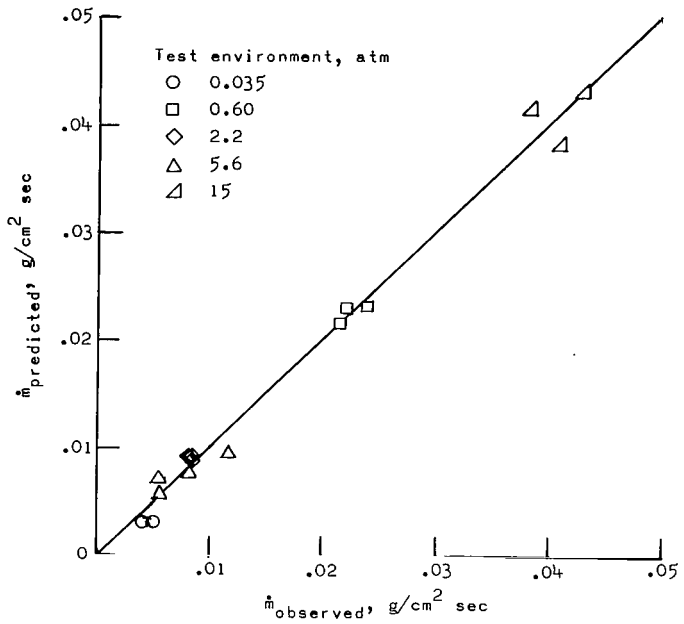

(a) LMSC Glass-like Carbon (eq. (1) of table IV).

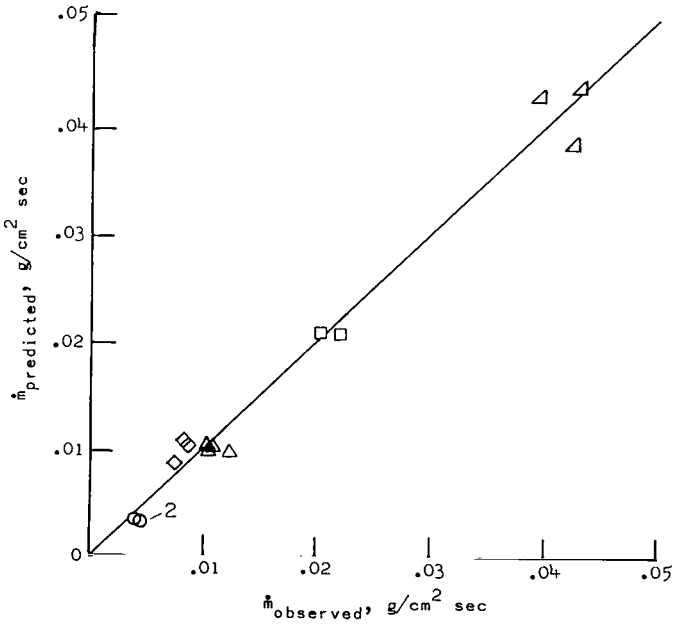

(b) Vitreous Carbon (eq. (2) of table IV).

Figure 10.- Comparison of predicted and observed mass-loss rates.

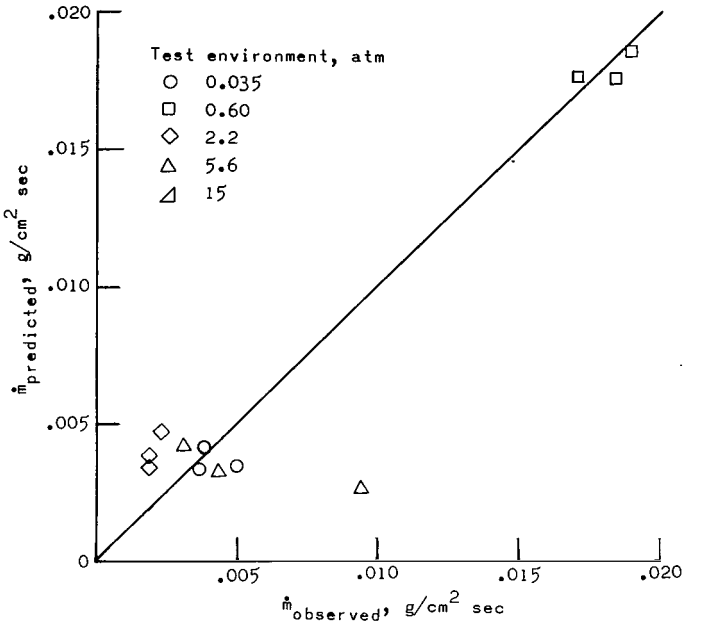

(c) Pyrolytic graphite (eq. (3) of table IV).

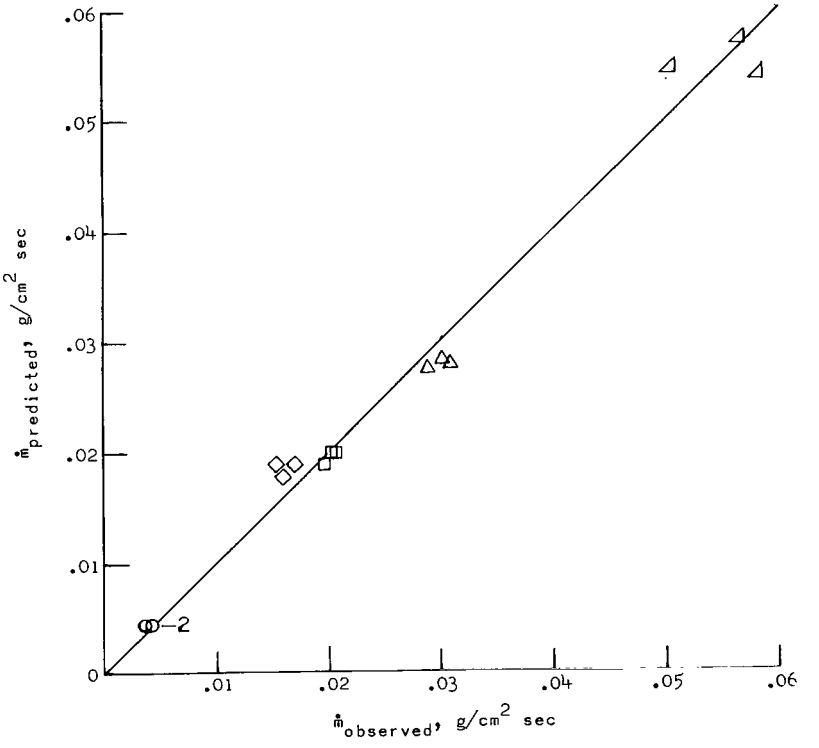

(d) ATJ graphite (eq. (4) of table IV).

Figure 10.- Continued.

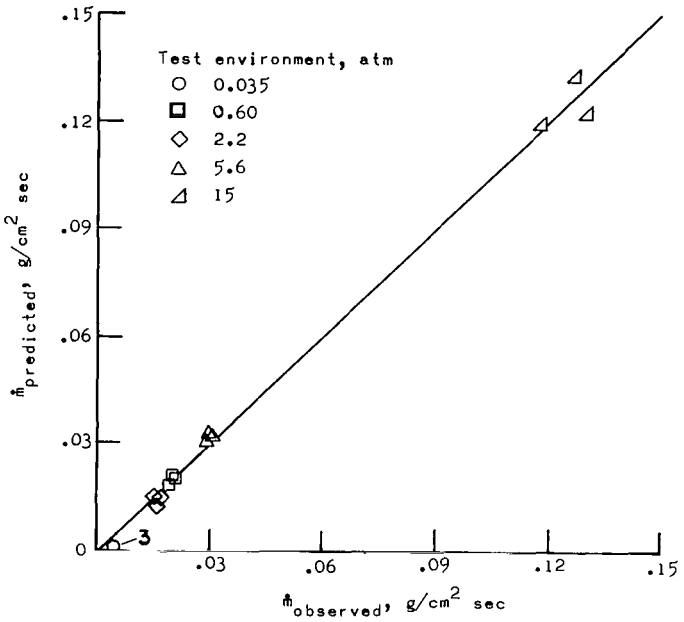

(e) ATJ graphite (eq. (5) of table IV).

Figure 10.- Concluded.

"The aeronautical and space activities of the United States shall be conducted so as to contribute . . . to the expansion of human knowledge of phenomena in the atmosphere and space. The Administration shall provide for the widest practicable and appropriate dissemination of information concerning its activities and the results thereof."

—NATIONAL AERONAUTICS AND SPACE ACT OF 1958

NASA SCIENTIFIC AND TECHNICAL PUBLICATIONS

TECHNICAL REPORTS: Scientific and technical information considered important, complete, and a lasting contribution to existing knowledge.

TECHNICAL NOTES: Information less broad in scope but nevertheless of importance as a contribution to existing knowledge.

TECHNICAL MEMORANDUMS: Information receiving limited distribution because of preliminary data, security classification, or other reasons.

CONTRACTOR REPORTS: Scientific and technical information generated under a NASA contract or grant and considered an important contribution to existing knowledge.

TECHNICAL TRANSLATIONS: Information published in a foreign language considered to merit NASA distribution in English.

SPECIAL PUBLICATIONS: Information derived from or of value to NASA activities. Publications include conference proceedings, monographs, data compilations, handbooks, sourcebooks, and special bibliographies.

TECHNOLOGY UTILIZATION PUBLICATIONS: Information on technology used by NASA that may be of particular interest in commercial and other non-aerospace applications. Publications include Tech Briefs, Technology Utilization Reports and Notes, and Technology Surveys.

Details on the availability of these publications may be obtained from:

SCIENTIFIC AND TECHNICAL INFORMATION DIVISION

NATIONAL AERONAUTICS AND SPACE ADMINISTRATION

Washington, D.C. 20546